Effect of Traps on Acoustoelectric Current Saturation in CdS*†

A. R. MOORE AND R. W. SMITH
RCA Laboratories, Princeton, New Jersey
(Received 28 December 1964)

Because of acoustoelectric interaction, the current-voltage (I-V) curve in the piezoelectric semiconductor CdS exhibits current saturation when the trap-controlled drift velocity equals the velocity of sound, and an internal acoustic flux is generated. By simultaneous measurement of the trap-controlled drift velocity from the I-V curve and of the Hall drift velocity over the temperature range 300 to 15°K, the effect of the traps in slowing down the velocity and frequency response of the electron-charge stream with respect to the internal acoustic flux is demonstrated. Comparison with a dynamical theory of trap occupation and space-charge bunching derived from the acoustic amplifier shows that the normal ionized donor states are the trapping agents, and that the effective angular frequency of the internal flux is 10^8 to 10^9 sec^{-1}. At very low temperatures, impact ionization of the donors is observed. The resulting enhanced current still flows at the sound velocity.

1. INTRODUCTION

IN their original papers on elastic wave propagation and amplification of ultrasonic waves in piezoelectric semiconductors, Hutson and White[1] and later White[2] showed that the propagation constants would be strongly modified by the presence of charge carriers and that amplification of an ultrasonic signal could be expected when the drift velocity $E\mu > v_s$, the velocity of sound in the medium. They also pointed out that the drift velocity should be interpreted as an effective drift velocity $f_0\mu_H E$, where μ_H is the ordinary Hall mobility and f_0 accounts for a possible division of the acoustically produced space charge between conduction band and bound states in the energy gap. This is because the electric field of an ultrasonic wave in a piezoelectric semiconductor can be neutralized by both bound and free charges, causing the creation of a periodic space charge through the medium (space-charge bunching). But the resulting conductivity modulation which enables the dc field to feed energy into the sound wave can only be effected by free charge. The result is that the drift field and the dc current must be raised just in the ratio f_0 of the free charge to the total space charge. In other words, the condition for amplification is $f_0\mu_H E \geq v_s$. It was assumed in their analysis that the bound charge, although bound in the sense of not contributing to conductivity, equilibrates with the conduction band in a time that is short compared with the frequency of the sound wave, i.e., the relaxation time $\tau \ll 1/\omega$.

Later authors[3–5] on the subject of amplification of ultrasonic waves in semiconductors generally ignored this possibility of trapped charge. Indeed, Hutson and White[6] themselves made no use of this concept in their experimental confirmation of ultrasonic amplification in CdS at room temperature. Greebe[7] pointed out the possibility of using the frequency dependence of the dc acoustoelectric effect to gain information about trapping levels. His proposed method, however, is hard to realize. Recently, Ishiguro, Uchida, Suzuki,[8] and Uchida, Ishiguro, Sasaki, and Suzuki (UISS)[9] have discussed theory and experiment of CdS ultrasonic amplifiers in which the limitation $\tau \ll 1/\omega$ no longer applies. We will return to their work shortly.

In experiments by Smith,[10] McFee,[11] and Moore,[12] it has been shown that an adequate measure of the drift velocity in semiconducting or photoconducting CdS crystals can be obtained very simply by measuring the current-voltage (I-V) curve. At a critical field E_c the current saturates as the drift velocity v_d equals the sound velocity. No acoustic energy need be introduced from outside the system. The saturation is presumably due to the internal generation of large-amplitude ultrasonic waves which by reason of the acoustoelectric interaction limit the carrier velocity to the wave velocity. Hutson[13] has attempted to account for this current saturation on the basis of acoustoelectric current flow counter to conduction current under amplifying conditions ($E\mu \geq v_s$) using the small-signal theory referred to above. This procedure is probably not completely valid because of the nonlinearity introduced by the strong coupling. Prohofsky[14] has offered another explanation based on generation of very high frequency

* The research reported in this paper was sponsored by the Advanced Research Agency, Materials Sciences Office, under Contract No. SD-182, and RCA Laboratories, Princeton, New Jersey.

† A preliminary report of part of this work was presented at the 7th International Conference on Semi-Conductors, Paris, July 1964, published as *Physics of Semiconductors* (Dunod Cie., Paris, 1964).

[1] A. R. Hutson and D. L. White, J. Appl. Phys. **33**, 40 (1962).
[2] D. L. White, J. Appl. Phys. **33**, 2547 (1962).
[3] K. Blötekajaer and C. F. Quate, Proc. IEEE **52**, 360 (1964).
[4] S. G. Eckstein, Phys. Rev. **131**, 1087 (1963).
[5] H. N. Spector, Phys. Rev. **127**, 1084 (1962); and **130**, 910 (1963).
[6] A. R. Hutson, J. H. McFee, and D. L. White, Phys. Rev. Letters **7**, 237 (1961).
[7] C. A. A. J. Greebe, Phys. Letters **4**, 45 (1963).
[8] T. Ishiguro, I. Uchida, and T. Suzuki, Paper presented at the 1964 IEEE International Convention, March 25, 1964 (unpublished).
[9] I. Uchida, T. Ishiguro, Y. Sasaki, and T. Suzuki, J. Phys. Soc. Japan **19**, 674 (1964), hereinafter referred to as UISS.
[10] R. W. Smith, Phys. Rev. Letters **9**, 527 (1962).
[11] J. H. McFee, J. Appl. Phys. **34**, 1548 (1963).
[12] A. R. Moore, Phys. Rev. Letters **12**, 47 (1964).
[13] A. R. Hutson, Phys. Rev. Letters **9**, 296 (1962).
[14] E. W. Prohofsky, Phys. Rev. **134**, A1302 (1964).

phonons (10^{10} to 10^{11} cps) by stimulated emission. Although the exact mechanism of the current saturation may not yet be understood, the strong interaction of carriers with the sound waves should still be expected to occur at the effective drift velocity $E\mu_d=v_s$.

In the present experiments, the relationship between the trap-controlled drift velocity determined from the I-V curves and the ordinary Hall velocity is examined as a function of temperature, internally generated sound frequency, and field.

2. THEORY OF THE EXPERIMENT

We assume a simple semiconductor model for the purpose of illustration: n-type semiconductor with a single donor and a single acceptor level. We also require a trapping level capable of temporarily trapping excited electrons from and re-emitting electrons into the conduction band. While the trap level, in principle, may be quite independent of the donor level, the results of the experiments indicate that an empty donor level itself acts as a shallow trap, and this is all we require. For simplicity we will initially assume that the trap relaxation time $\tau \ll 1/\omega$, where ω is the dominant acoustic frequency.

The Hall mobility $\mu_H=R_H\sigma$ and the corresponding Hall drift velocity $v_{dH}=R_Hj$ are thermal equilibrium quantities and hence trap-independent. The drift mobility obtained from acoustoelectric current saturation is a measure of the velocity under unit electric drift field of the carriers bunched in the local piezoelectric field of the internally amplified sound waves. These bunched carriers are excess above the local thermal equilibrium value and as such may be considered excited or injected carriers. Their mobility may be reduced if they spend appreciable time in traps during their transit time through the crystal. Using the same approach as is used for the photoexcited electrons in a photoconductive sample[15] we may express the relationship between the trap-controlled drift mobility μ_d^* and the ordinary Hall mobility μ_H as

$$\mu_d^*=\mu_H(n/(n+n_t)), \tag{1}$$

where n and n_t are the densities of free and trapped carriers, respectively. The acoustically produced space charge may be expected to divide in the same way between free and trapped states even if the acoustic space charge does not constitute all the charge, although the very strong current saturation observed leads us to believe that most of the available charge is in fact acoustically limited. Thus the factor f_0 from the acoustic amplifier theory is just μ_d^*/μ_H. In terms of τ_f, the time an electron is free to move in the conduction band, and τ_t, the time it spends in a trap, f_0 becomes

$$f_0=\mu_d^*/\mu_H \tag{2a}$$

$$f_0=1/(1+(n_t/n))=1/(1+(\tau_t/\tau_f)). \tag{2b}$$

For a single trap level in communication with the conduction band this can also be written

$$f_0=[1+(N_t/N_c)e^{E_t/kT}]^{-1}, \tag{3a}$$

which is equivalent to taking

$$\tau_f=(1/N_tv_{\rm th}S) \quad \text{and} \quad \tau_t=(e^{E_t/kT}/N_cv_{\rm th}S). \tag{3b}$$

In Eqs. (3a) and (3b) N_c is the conduction-band density of states ($4.24\times10^{14}T^{3/2}$ for CdS with $m^*/m=0.2$), N_t is the trap density, $v_{\rm th}$ is thermal velocity, S is the capture cross section, and E_t is the trap depth below the conduction band. If in the simple semiconductor model assumed at the outset, $N_D-N_A\ll N_A$, N_D (i.e., heavily compensated), then $N_t\approx N_A\approx N_D$ and $E_t=E_d$, the donor activation energy; the ionized donor states act as electron traps.

We have indicated that current saturation of the I-V curve occurs at a critical electric field E_c such that $f_0\mu_HE_c=\mu_d^*E_c=v_s$. The saturated current density j can also be evaluated. In general

$$j=nev=neE\mu_H. \tag{4}$$

In terms of Eqs. (1) or (2) this can also be written

$$j=neE\mu_d^*/f_0=(n+n_t)eE\mu_d^*. \tag{5}$$

Using the condition for saturation $j=j_{\rm sat}$, when $\mu_d^*E_c=v_s$

$$j_{\rm sat}=nev_s/f_0=(n+n_t)ev_s. \tag{6}$$

We can now remove the restriction $\tau\ll1/\omega$ and instead assume $\tau\approx1/\omega$. The acoustically produced periodic space charge can be thought of as two streams of bunched charge, one mobile, the other bound to electron-trapping centers. As long as the relaxation time of the trapping $\ll1/\omega$ the two streams are coincident in space and time and the ratio of the free charge to the total is given by f_0 [Eq. (2)]. When $\tau\approx1/\omega$ a phase difference develops which is best expressed by considering the two streams as in dynamical equilibrium, which leads to f_0 becoming a complex quantity f. UISS have given a satisfactory description of this situation as it pertains to the acoustic amplifier at room temperatures, in which τ is taken as a fixed quantity. In our experiments the temperature is varied over a wide range, and it is important to know something about the temperature dependence of τ. Furthermore, τ does not appear explicitly in our formulation; rather we have expressed f_0 in terms of τ_t and τ_f. The appropriate rate equation for the rate of change of trapped charge in terms of the interchange between trapped and free charge is

$$dn_t/dt=-(n_t/\tau_t)+(n/\tau_f). \tag{7}$$

If $dn_t/dt=0$, $n_t/n=\tau_t/\tau_f$ which leads to the dc solution [Eq. (2)]. Take the total charge $n_t+n=N$. In the dynamical or ac state, define $f=n/N$ and $1-f=n_t/N$,

[15] See, for example, R. Bube, *Photoconductivity* (John Wiley & Sons, Inc., New York, 1960), p. 68.

analogous to Eq. (2). Assuming a sinusoidal solution for N

$$N=N_0e^{i\omega t}, \tag{8}$$

we obtain from Eq. (7) a complex form for f:

$$f=\frac{\tau_f(1+i\omega\tau_f)}{\tau_f+\tau_t+i\omega\tau_t\tau_f}. \tag{9}$$

Since Eq. (2) relates f_0, τ_t, and τ_f, we may write Eq. (9) in terms of either τ_t or τ_f

$$f=\frac{(1+i\omega\tau_t)f_0}{1+i\omega\tau_tf_0}=\frac{f_0+i\omega\tau_f(1-f_0)}{1+i\omega\tau_f(1-f_0)}. \tag{10}$$

If we now set

$$\tau=\tau_f\tau_t/(\tau_f+\tau_t), \tag{11}$$

Eqs. (9) and (10) can be consolidated into a single form

$$f=((f_0+i\omega\tau)/(1+i\omega\tau)), \tag{12}$$

which is equivalent to the solution given by UISS. Equation (11) shows, however, that the dynamical system relaxes through both τ_t and τ_f acting in parallel, the shorter of the two dominating. This, taken with Eq. (3b), enables the calculation of the variation of τ with temperature, which is important in the analysis of our experiments and to which we will return later.

It proves convenient to express the complex factor f in terms of two other functions

$$f=(bf_0/(1-ia)), \tag{13a}$$

where

$$a=((1-f_0)\omega\tau/(f_0+\omega^2\tau^2)) \tag{13b}$$

and

$$b=((f_0^2+\omega^2\tau^2)/f_0(f_0+\omega^2\tau^2)). \tag{13c}$$

The function a is just the ratio of the imaginary to the real part of f and therefore measures the phase shift of the free charge relative to the total acoustically produced space charge.

If f is substituted back into the Hutson and White analysis, all the equations of the ultrasonic amplifier can be obtained, suitably modified by the functions a and b containing the relaxation time. UISS have given the essential equations for acoustic gain. We shall not repeat them here because our experiments do not measure gain directly and, in any case, the results are possibly misleading, since they are based on the small-signal theory. But just as the low-frequency ($\omega\tau\ll1$) small-signal theory does predict correctly that strong energy transfer from conduction current to sound waves begins at the effective drift velocity $f_0\mu_HE_c=v_s$, so we may expect that it will also predict the correct analogous result when $\omega\tau\gtrsim1$. The equation for the effective drift velocity under these conditions becomes simply

$$v_d^*=bf_0\mu_HE \tag{14a}$$

or

$$\mu_d^*=bf_0\mu_H, \tag{14b}$$

with b defined as in Eq. (13c). Saturation occurs, as before, when $E=E_c$, $v_d^*=v_s$

$$v_d^*=bf_0\mu_HE_c=\mu_d^*E_c=v_s. \tag{15}$$

When $\omega\tau\ll1$, $b=1$, $f=f_0$ and $\mu_d^*=f_0\mu_H$ as in Eq. (2). The phase shift $\tan^{-1}a$ is zero. In the intermediate case $\omega\tau\approx1$, $b>1$, $f>f_0$ and $\mu_d^*>f_0\mu_H$. A phase shift develops between free charge and total acoustically produced space charge due to the relaxation time of the trapping. Finally, when $\omega\tau\gg1$ the free charge can no longer remain in communication with the trapped charge and the effect of the traps in reducing the drift mobility disappears. Then $b=1/f_0$, $f=1$, and $\mu_d^*=\mu_H$. The phase shift again goes to zero.

We can apply these ideas to the saturated current density by simply replacing f_0 by bf_0 in Eq. (6).

$$j_{\rm sat}=(nev_s/bf_0)=((n+n_t)/b)ev_s. \tag{16}$$

If we let $j_{\rm sat}=j_{\rm sat_0}$ for $\omega\tau\ll1$ when $b\rightarrow1$

$$j_{\rm sat}/j_{\rm sat_0}=1/b, \tag{17}$$

and combining Eq. (14b) with Eq. (17)

$$(\mu_d^*/\mu_H)(j_{\rm sat}/j_{\rm sat_0})=f_0. \tag{18}$$

Equation (18) should hold over all values of $\omega\tau$, in contrast to Eq. (2a) which holds only for $\omega\tau\ll1$. In the following experiments and analysis it is assumed that ω is a constant of the crystal, independent of temperature. However, because the acoustic gain mechanism is inherently rather broad band, we expect in reality that the internal acoustic flux generated will have a considerable spread in frequency. Our value of ω is then to be taken as the dominant or maximum in this frequency distribution.

3. EXPERIMENT AND DISCUSSION

a. Materials and Methods

Most of the data presented here were taken on samples of Eagle-Picher CdS "UHP" crystals cut from boules and polished optically flat on all sides. The samples were typically 0.5×0.5×0.5 mm, although those used for Hall effect and absolute conductivity measurements were longer (1 to 2 mm) to accommodate the required additional electrodes. Most samples had room-temperature resistivities in the range 1–10 Ω-cm. Indium electrodes were applied on the lightly etched polished surfaces by evaporation through suitable copper masks to accurately define their position and dimensions. Thick layers are desirable for good ohmic contact. The crystals were usually oriented so that $E\|c$, although saturation can also be obtained[10] with $E\perp c$.

All I-V curves were taken by pulse methods, using a high-current, high-voltage pulser, with low repetition

rate to avoid heating, and pulse width about 10 μsec. Pulse current was measured by an inductive current pickup, Tektronix No. P6016, which eliminates the necessity for a series resistance in the current path. The low-current Hall measurements were obtained by conventional dc methods, using a vibrating-reed electrometer for the Hall voltage and potential drop. The high-current Hall measurements were done by pulse methods, utilizing differential input to the oscilloscope preamplifier through high-impedance probes.

Temperature variation was accomplished by mounting the sample in one of two simple cryostats, depending on the temperature range, both using helium-exchange gas. For the room-temperature to liquid-nitrogen range, the sample was cooled by circulating precooled helium around the sample mounted on a copper block at the end of a stainless-steel tube. Temperature was adjusted by changing the helium-flow rate. For the lower temperature range down to 4°K, the second cryostat was used in which the sample was mounted inside an evacuable copper can immersed in liquid helium. Temperature was controlled by the thermal balance between the heat input to a resistor wound on the sample block and the heat loss to the adjustable helium ambient inside the can. Thermocouples and/or carbon resistance thermometers were used to monitor sample temperature. Although a sample temperature only slightly above liquid helium could easily be reached, it was not possible to obtain reliable low-current Hall and resistivity measurements much below 15°K. The measurement became erratic, not so much because of high bulk resistance, but because the contacts became non-Ohmic with very high contact resistance. This difficulty apparently is not as serious in the simple pulsed I-V curves in which the contacts are carrying higher currents.

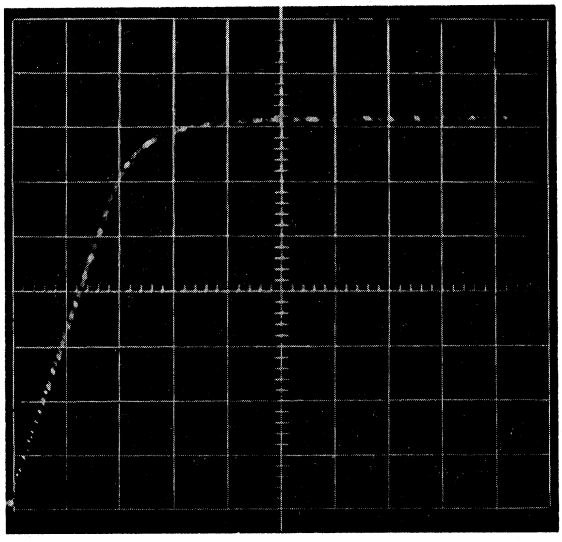

FIG. 1. Typical room-temperature I–V curve for a sample of semiconducting CdS. The critical field for current saturation (extrapolated intersection of the ohmic and saturation portions of the curve) occurs at 1500 V/cm.

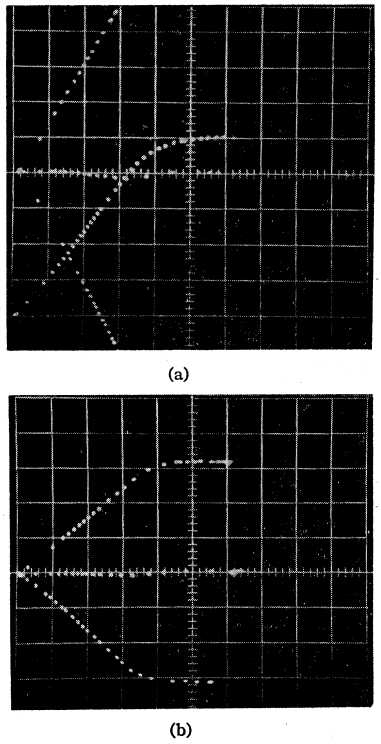

(a)

(b)

FIG. 2. Comparison of I–V and Hall-voltage versus applied-voltage curves for a semiconducting CdS sample at room temperature. (a) I–V curve (lowest curve). The three upper curves show Hall voltage versus applied voltage for magnetic field of +5 kG, 0 kG, and −5 kG. (b) Hall voltage versus applied voltage for magnetic fields of +5 kG, 0 kG, and −5 kG. Applied-voltage scale same as in (a) above. Curve shows Hall drift velocity saturating at 4×10^6 cm/sec.

b. Results above 77°K

Figure 1 shows a typical room-temperature I-V curve for a sample of semiconducting CdS, $\sigma\approx0.5(\Omega\text{-cm})^{-1}$, $E\|c$, as observed directly on the x-y oscilloscope. Each dot represents a single pulse, the entire curve being traced out as a series of dots as the pulse voltage is slowly increased. Ohm's law is obeyed up to several amperes which corresponds to current densities of a few hundred amperes per square centimeter. Strong current saturation is then observed. The critical field E_c was obtained by simple extrapolation of the Ohm's law and saturation current sections of the curve.

Figure 2(a) shows the I-V curve on another similar sample which had attached the additional electrodes needed for Hall-voltage and potential-drop measurements. The lowest curve is the I-V curve. The set of three upper curves is the Hall voltage versus applied voltage for magnetic field equal to +5000, 0, and −5000 G. Since $V_H\sim R_H I/B$, the Hall drift velocity $v_{dH}=R_H j\sim V_H$. The balance between the inputs from the Hall contacts to the differential amplifier was

adjusted in each sample and at each temperature so that the best zero line at zero magnetic field was obtained. Slight deviations as a function of applied voltage were always observed due to the relatively high pulse voltage on each contact compared with the much smaller Hall voltage difference between them. Slight nonlinearities in different sections of the crystal are therefore much magnified. The example shown is one in which the deviation was smaller than usual. In any case, true Hall voltage was obtained as the average of $+B$ and $-B$ curves which should cancel out this zero drift.

Figure 2(a) shows that the Hall drift velocity is linear as long as the I-V curve is Ohmic. Figure 2(b) with a less sensitive Hall-voltage scale clearly shows that v_{dH} saturates just when the I-V curve saturates. Again we plot the Hall voltage for ± 5000 G and 0 G. The Hall voltage was always linear with magnetic field.

Figure 3 shows data at room temperature and 77°K converted to absolute current density, electric field, and Hall drift velocity for the same samples as Fig. 2. The room-temperature Hall drift velocity saturates at 4×10^5 cm/sec which is very close to the known velocity of longitudinal sound waves in CdS, 4.3×10^5 cm/sec. The critical saturation field is about 1300 V/cm, giving $\mu_d^*=v_s/E_c=330$ cm²/Vsec. Combining v_{dH} from the linear part of the curve with σ from the corresponding portion of the j-E curve yields $\mu_H=330$ cm²/sec. Thus at 300°K, $\mu_H=\mu_d^*$.

At 77°K, E_c is only 250 V/cm, yielding $\mu_d^*=1700$ cm²/Vsec. The corresponding Hall mobility from the linear portion is 3600 cm²/Vsec. Thus at 77°K, μ_H is not equal to μ_d^*. The saturated value of v_{dH} is larger than the sound velocity in the ratio that the Hall mobility bears to the drift mobility, as expected from Eq. (2a). Also, we commonly observe that the saturation current changes very little from 300–77°K, as can be seen in Fig. 3, although E_c may decrease markedly by a factor as large as three to six for different samples.

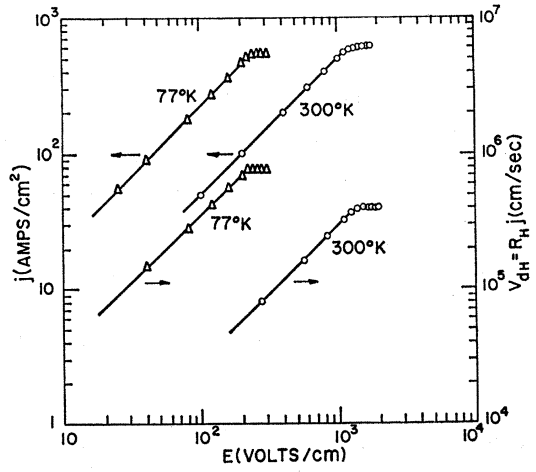

FIG. 3. Curves of current density j and Hall drift velocity v_{dH} versus E for room temperature and liquid-nitrogen temperature.

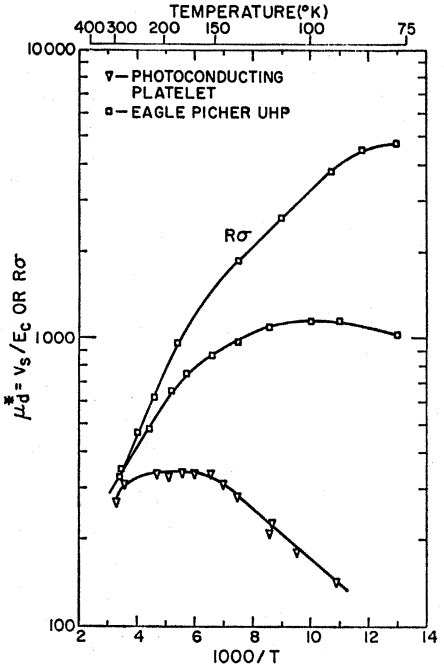

FIG. 4. Drift mobility as a function of $1/T$ for a semiconducting (Eagle-Picher UHP) and a photoconducting (RCA) sample.

Saturation current independent of temperature is consistent with Eq. (6), which shows that j_{sat} depends on $(n+n_t)$. As the temperature is lowered electrons become bound to donors (the Hall coefficient rises), but since they must be either free or trapped $(n+n_t)$ remains constant.

The effect of trapping on the drift mobility is shown more clearly in Fig. 4, which gives $\log\mu_d^*$ as a function of $1/T$ in the 300–77°K temperature range for a typical semiconductor sample. Also shown are the Hall mobility data for this same sample, determined in this case by dc low-current methods since previous work had indicated that there was no appreciable difference between dc and high-current pulse Hall mobility in the Ohmic range. For comparison, we present data on μ_d^* for an insulating platelet sample, rendered conducting by strong illumination. The photoconductors vary widely from sample to sample, while most semiconducting specimens we have examined are rather similar. For the latter, the Hall and drift mobility agree well at 300°K but show increasing deviation as the temperature is lowered to 77°K. The deviation is larger for photoconducting samples. According to Eq. (3a), derived on the basis of a single trap level, $\log[\mu_H/\mu_d^*-1]T^{3/2}$ versus $1/T$ should yield the parameters of the trapping system E_t and N_t as the slope and intercept, respectively. Figure 5 shows this plot for the two samples of Fig. 4. A trap level of 0.017 eV and density of 1.3×10^{17}/cm³ was obtained for the semiconducting sample, a trap level of 0.025 eV and density 4.2×10^{17}/cm³ for the insulating photoconductor.

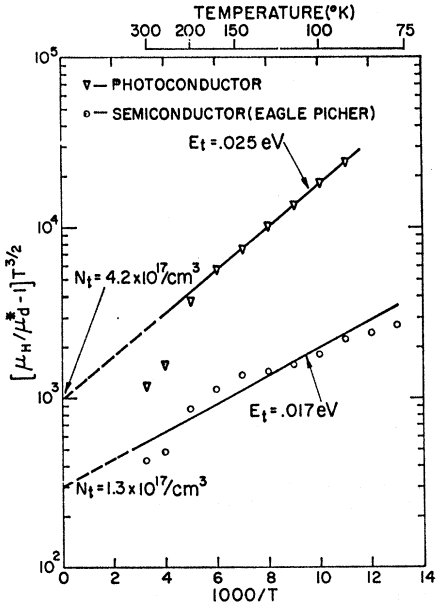

FIG. 5. $(\mu_H/\mu_d^*-1)T^{3/2}$ versus $1/T$ above 77°K for the two samples of Fig. 4.

c. Results Down to 20°K

Extension of the results reported in Sec. 3b down to lower temperatures enables a number of important tests of the trapping theory. The Hall coefficient versus temperature curves for semiconducting samples yield donor activation energies of 0.015±0.002 eV, the free-electron concentration at room temperature $n_0 \approx N_D - N_A$ is in the range of 10^{15} to 10^{16}/cm^3, and the acceptor concentration is $\sim 10^{17}$/cm^3. Typical Hall coefficient and Hall mobility data are shown in Figs. 6(a) and (b). The corresponding drift mobility data obtained from *I-V* curves are presented in Fig. 7, in which the ratio μ_d^*/μ_H is plotted against T for two samples of slightly different impurity concentrations. The important point here is that μ_d^*/μ_H decreases with temperature due to trapping, but at sufficiently low temperature the effect of the trapping disappears due to the inability of the free charge to come into equilibrium with the trapping state. Then μ_d^* again becomes equal to μ_H, that is, $bf_0 \rightarrow 1$. This produces the observed minimum.

Similarly, for the low-temperature range (<77°K) the saturation current [Eq. (16)] is no longer independent of temperature, since it contains the factor b [Eq. (13c)] which is temperature-dependent below the point where $f_0 \approx \omega\tau$. In Fig. 8, we plot experimental values of j_{sat} relative to the saturation current at room temperature j_{sat_0}. The ratio is relatively constant above 77°K, but falls very sharply at lower temperature, in accordance with Eq. (17).

From an experimental point of view, we may make a direct determination of f_0 through Eq. (18). The product $(\mu_d^*/\mu_H)(j_{sat}/j_{sat_0})$ cancels out the effect of $\omega\tau$, since μ_d^*/μ_H is increased by the departure of the free charge from equilibrium by the same ratio as the saturation current is decreased. This plot is shown in Fig. 9(a). Finally utilizing Eq. (3a) which relates trap depth to f_0, we plot $\log[(1/f_0)-1]T^{3/2}$ versus $1/T$, f_0 being determined as in Fig. 9(a). The result is shown in Fig. 9(b). This plot is directly analogous to Fig. 4. It has the advantage that a much wider range of reciprocal temperature can be employed resulting in a more reliable value of the trap depth. From the graph, we estimate $E_t=0.014$ eV and $N_t=1.2\times10^{17}$/cm^3, which

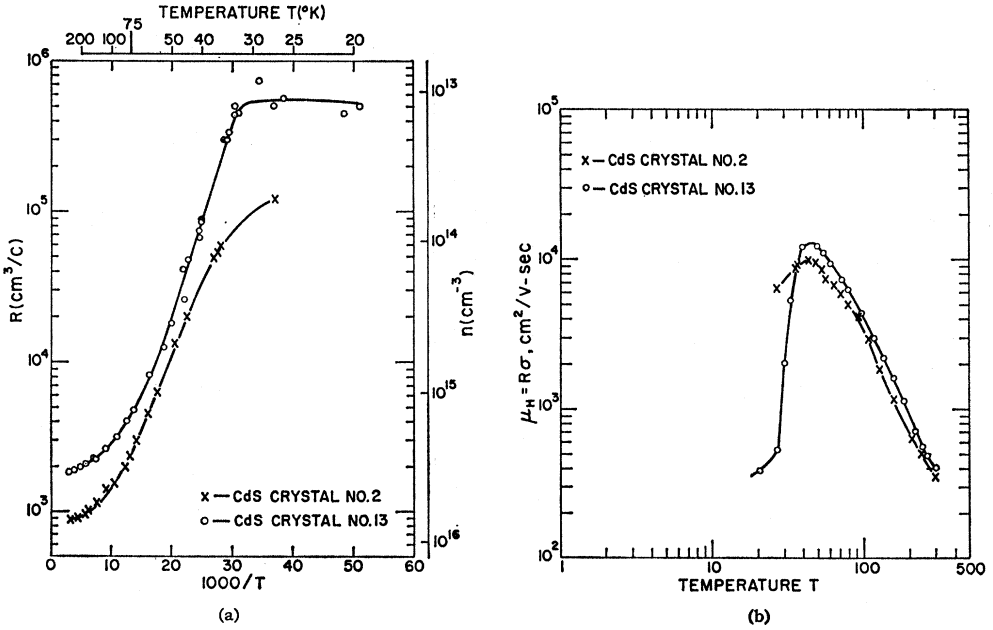

FIG. 6. Hall data on two semiconducting CdS samples down to~20°K. (a) Hall coefficient versus $1/T$. (b) Hall mobility $\mu_H = R_H\sigma$ versus T.

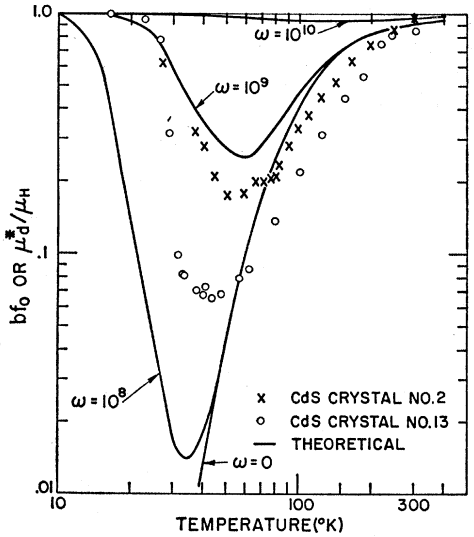

FIG. 7. Experimental points: μ_d^*/μ_H versus T for the two samples of Fig. 6. The solid line is a theoretical curve plotting bf_0 versus T for a choice of the parameter ω [Eq. (13c)].

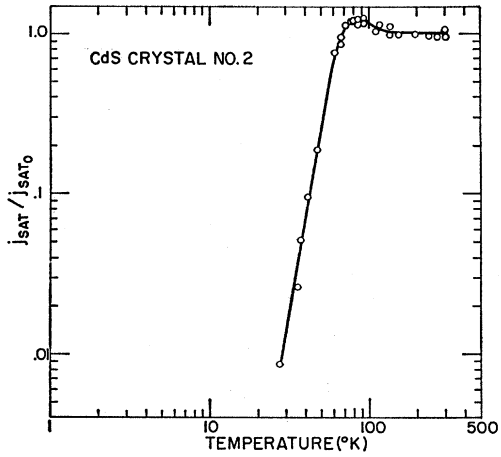

FIG. 8. Experimental value of j_{sat} relative to the saturation current density at room temperature j_{sat_0}.

is in good agreement with the donor activation energy 0.015 eV and $N_A=8\times10^{16}/\text{cm}^3$ obtained from the Hall coefficient.

d. Comparison with Trapping Theory

The foregoing results establish that the single-level semiconductor model gives a qualitative explanation for the variation of the drift mobility with temperature. In order to make a quantitative comparison it is necessary to know ω and τ. The sound frequency is an unknown because it is internally generated. The present experiments give directly only the ratio τ_t/τ_f from f_0, rather than τ itself. In order to use our data to obtain a value for ω, as well as provide a test for the trap theory, we proceed directly to estimate τ_t and τ_f separately from Eq. (3b). The trap depth and concentration are already known. The only unknown is the cross section for recombination of an electron with the trapping (donor) center. The problem of recombination of electrons with donors has been treated theoretically by several authors. Rose[16] gives an elementary derivation showing that $S\sim T^{-2}$. Ascarelli and Rodriguez[17] made a detailed calculation for Ge doped with As($E_d=0.0127$ eV) which agreed well with experimental values. They found $S\sim T^{-2.5}$ below 6°K tending toward T^{-2} above 6°. Since E_d, mean effective mass,

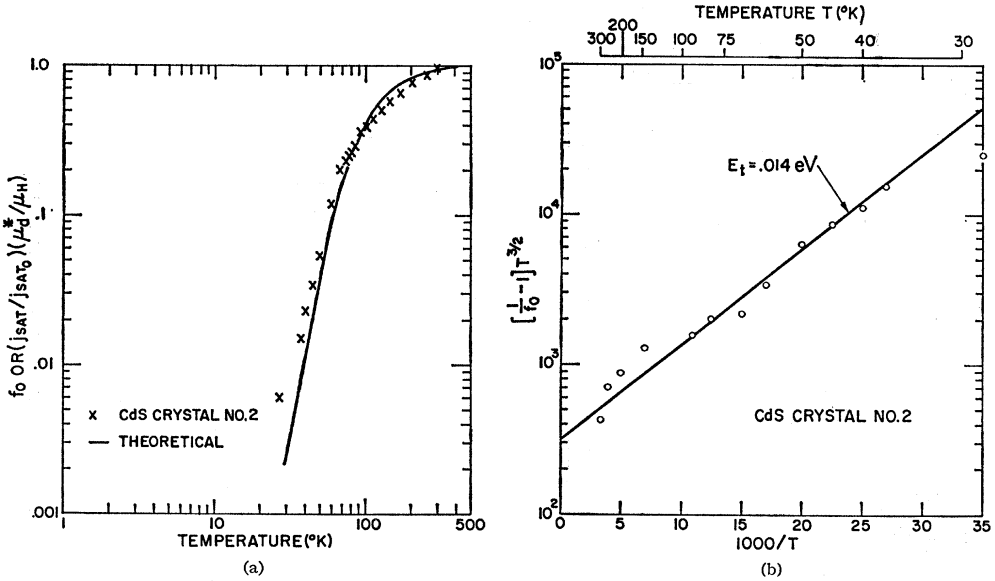

FIG. 9. (a) Experimental values of (μ_d^*/μ_H) (j_{sat}/j_{sat_0}) as a function of temperature. The solid line is a theoretical curve of f_0 versus T [Eq. (2b)]. (b) log $[(1/f_0)-1]T^{3/2}$ versus $1/T$.

[16] A. Rose, *Concepts in Photoconductivity* (Interscience Publishers, Inc., New York, 1963) p. 123.
[17] G. Ascarelli and L. Rodriguez, Phys. Rev. **124**, 1321 (1961).

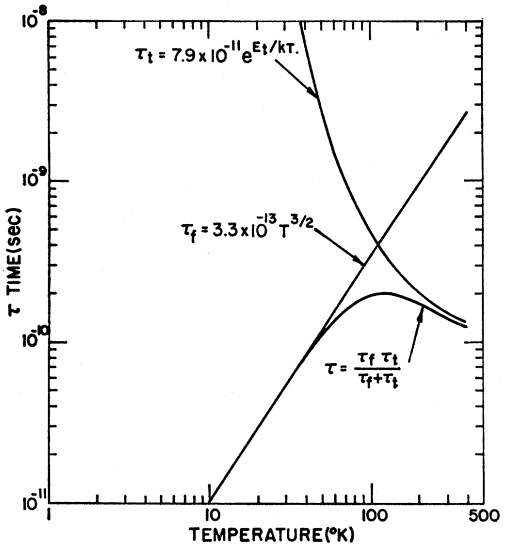

FIG. 10. Free time τ_f and trapping time τ_t versus temperature [Eq. (3b)]. $E_t=0.015$ eV and $S=3.6\times10^{-11}T^{-2}$. The combination $\tau_f\tau_t/(\tau f+\tau_t)$ gives the relaxation time τ [Eq. (11)].

and dielectric constant are all similar for the CdS case, we have taken their result in the approximate form $S=3.6\times10^{-11}T^{-2}$, together with the value of $E_d=0.015$ eV and $N_t=10^{17}/\text{cm}^3$ obtained in the present experiment on CdS to construct τ_f, τ_t, and τ versus T curves from Eqs. (3b) and (11). This is shown in Fig. 10. The solid line in Fig. 9(a) is the computed value of f_0 versus T which is in fairly good agreement with experiment. Actually, the recombination cross section S is not used in the computed values of f_0 in Fig. 9(a) because it cancels out in the ratio τ_t/τ_f. It is used, however, in the calculated curves of Fig. 7 which plot bf_0 [Eqs. (13c) and (14b)] versus T with ω as a parameter. The general shape of the curve reproduces the experimental values of μ_d^*/μ_H fairly well for choice of ω between 10^8 and 10^9 cps. The minimum in Fig. 7 occurs at the temperature at which $\omega\tau\approx f_0$. This is a better criterion for the existence of relaxation effects due to trapping than $\omega\tau\approx1$ used earlier, in the case that $f_0\ll1$.

UISS were able to make an estimate of τ from the gain characteristics of an acoustic amplifier independent of assumptions other than the trapping theory itself because the acoustic frequency ω was known; on the other hand, they could not estimate E_t. They obtained $\tau\approx10^{-8}$ sec at room temperature. The rather smaller value $\tau\approx10^{-10}$ sec (see Fig. 10) used here is not to be taken as disagreement between us. The variance is due entirely to the different nature of the crystals. Our semiconducting samples are relatively heavily doped, as the small values of donor activation energy readily shows. The highly photosensitive, low dark current, highly compensated crystals used by UISS would be expected to have longer relaxation time. In other respects the two types of measurements complement each other.

e. Impact Ionization

At low temperatures when $\omega\tau\gg f_0$ and $bf_0\approx1$, the saturation current falls to low values because of deionization of the donors. However, if the electric field is increased much beyond that needed to obtain saturation the current begins to rise again. This is shown in Fig. 11. The I-V curves are given for several temperatures between 300 and 4°K. We plot log$I$ versus V in order to bring out the voltage region in which the current rises beyond the saturation, although the relatively sharp onset of the saturation itself is somewhat suppressed. A careful investigation of Hall voltage and conductivity within this voltage region has shown without doubt that impact ionization of impurities leads to the enhanced current at low temperatures. The carrier density increases with increasing voltage until all the donors have been ionized. Then current saturation again sets in. The magnitude of this second saturation current at low temperature is approximately equal to the ordinary saturation at high temperature. Measurement of the Hall drift velocity, which in this low-temperature range is equal to the actual drift velocity ($bf_0\approx1$), shows that v_{dH} is saturated at the velocity of sound over the entire range. Thus, once the velocity of sound is reached, carriers maintain this velocity during the impact-ionization "breakdown."

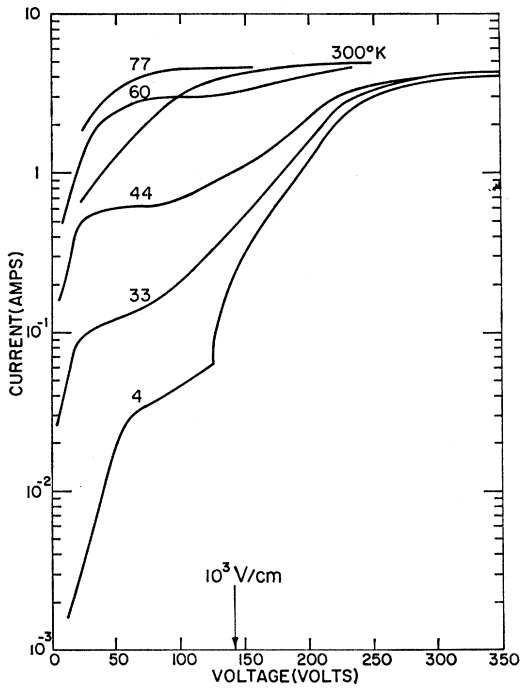

FIG. 11. Log I-V curves at various temperatures for a semiconducting CdS crystal. At temperatures below 77°K, impact ionization of impurities can be observed.

The result poses an interesting problem: The donor ionization energy of 0.015 eV would seem to require a drift velocity of 10^6 to 10^7 cm/sec in order to ionize by collision, yet apparently ionization can already occur at the velocity of sound. A difference between measured average drift velocity and calculated velocity needed for ionization is usually accounted for[18] by arguing that the onset of breakdown is due to those charge carriers on the high-energy side of the carrier energy distribution rather than to those having the average value. In our case, due to the strong piezoelectric interaction in CdS, the measured average velocity must be the velocity of most carriers. The normal velocity distribution piles up against the "sound barrier." Yet the fact that impact ionization of impurities is observed implies that some carriers escape through the barrier to maintain the ionization rate. The finite slope of the saturation curve at 77°K implies that a few percent of such carriers exist. We believe this may be the explanation for the fact that the breakdown is not precipitous as it is in germanium. The relatively low ionization rate evidenced by the rather slow rise of current with field would then be explained by imagining that most of the carriers, locked at sound velocity, never take part in ionization at all. Most additional carriers created by the few fast electrons become similarly velocity-limited. In effect, the ionization rate is reduced by the ratio of fast to sound-limited electrons.

This idea also offers an explanation for the rapid current rise observed only at the lowest temperatures (4°K and in some crystals) at the beginning of the impact-ionization region. Here the carrier density is so low that the acoustoelectric gain in the sense of Hutson and White is much reduced. The normal current saturation is weak because the acoustic amplitude cannot grow. When the breakdown point is finally reached, most carriers not limited to v_s take part in the ionization and the carrier density rises with a large ionization rate. A point is soon reached, however, where the carrier density is sufficiently large to allow the generation of the large-amplitude acoustic waves needed to lock the distribution back to the sound velocity. The ionization rate is then reduced and the current rises with voltage at approximately the same rate as for higher temperatures. Unfortunately, we have not been able to make a detailed check on this speculation because of the difficulty of making reliable pulse Hall measurements at 4°K in CdS.

[18] N. Sclar and E. Burstein, J. Phys. Chem. Solids 2, 1 (1957).

4. CONCLUSIONS

The sum of the theory and experiment presented is that the *I-V* curves of semiconducting CdS are profoundly affected by the generation of acoustic waves and the presence of shallow traps. The shape of the curves, when interpreted in terms of the electron drift velocity, is well explained by a single-level trap theory which takes into account the relaxation time of electrons in the trap, in cooperation with the theory of the piezoelectric ultrasonic amplifier. The ionized donor levels of the compensated semiconductor comprise the trap system. When the drift velocity (measured in such a way as to take into account the time electrons spend in the traps) equals the velocity of sound, the current saturates. This saturation is accompanied by the generation of acoustic waves of angular frequency ω in the range 10^8–10^9 sec^{-1}. This is in agreement with the frequency of the ultrasonic flux buildup observed by McFee[11] with the use of a transducer ($15<\omega/2\pi<400$ Mc/sec) and of Blotekjaer and Quate[3] by observation of the rf crystal current ($90<\omega/2\pi<450$ Mc/sec). Both these experiments were done with high-resistance photoconducting crystals. If the internally generated sound is built up from thermal noise by a mechanism following the small-signal gain equations of Hutson and White, one would expect the dominant frequency to be in the neighborhood of the peak of the gain versus frequency curve, which for our crystals is $\omega_{\max}=(\omega_C\omega_D)^{1/2}\approx 10^{11}$ sec^{-1}. The Prohofsky stimulated-emission theory also predicts generation of phonon waves in the same frequency range. Our result, which indicates frequencies two to three orders of magnitude lower, is apparently in disagreement with these theories. It is possible that the mechanism postulated by Hutson for the acoustoelectric current could be brought into line with our data, if the fact that the electron drift velocity cannot exceed the sound velocity by but a very small amount were taken into account. Then the value of $\gamma=1-v_d^*/v_s$ would remain very close to zero even under amplifying conditions. The intersection of the gain versus frequency curve with the Akhiezer ω^2 loss curve would then be shifted far toward the direction of lower frequencies, perhaps leaving a net gain curve which peaks at 10^8 to 10^9 sec^{-1}, with a weaker dependence on $\omega_{\max}$ and hence on crystal resistivity.

5. ACKNOWLEDGMENTS

We wish to thank C. Oldakowski and B. Tompkins for aid in construction of equipment and taking of data. We have also benefited greatly from discussions with A. Rose and M. Lampert.

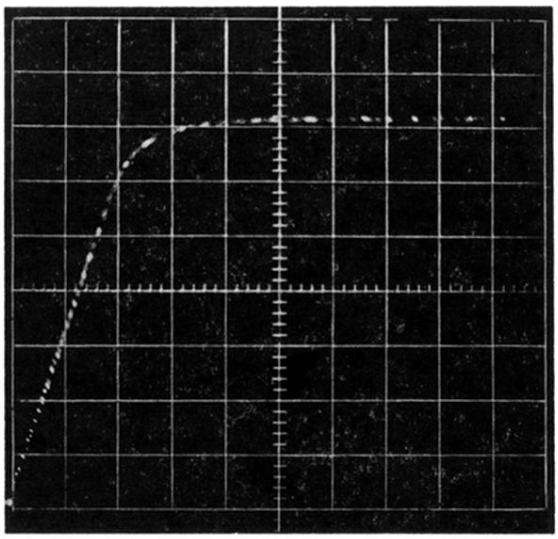

FIG. 1. Typical room-temperature I–V curve for a sample of semiconducting CdS. The critical field for current saturation (extrapolated intersection of the ohmic and saturation portions of the curve) occurs at 1500 V/cm.

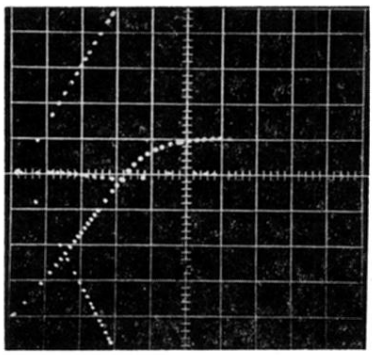

(a)

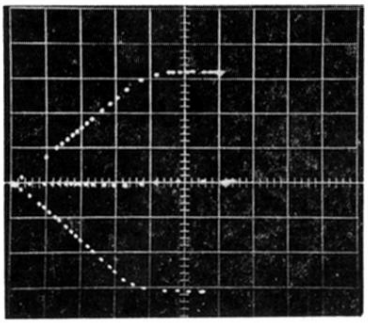

(b)

FIG. 2. Comparison of I–V and Hall-voltage versus applied-voltage curves for a semiconducting CdS sample at room temperature. (a) I–V curve (lowest curve). The three upper curves show Hall voltage versus applied voltage for magnetic field of $+5$ kG, 0 kG, and -5 kG. (b) Hall voltage versus applied voltage for magnetic fields of $+5$ kG, 0 kG, and -5 kG. Applied-voltage scale same as in (a) above. Curve shows Hall drift velocity saturating at 4×10^5 cm/sec.